LAWRENCE
LIVERMORE
NATIONAL
LABORATORY

LLNL-JRNL-521754

A counterflow diffusion flame study of lightly branched octane isomers

S. M. Sarathy, U. Niemann, C. Yeung, R. Gehmlich, C. K. Westrbrook, M. Plomer, Z. Luo, M. Mehl, W. J. Pitz, K. Seshadri, M. J. Thomson, T. Lu

January 2, 2012

Proceedings of the Combustion Institute

Disclaimer

Elsevier Editorial System(tm) for Proceedings of the Combustion Institute
Manuscript Draft

Manuscript Number:

Title: A counterflow diffusion flame study of lightly branched octane isomers

Article Type: Research Paper

Keywords: 3-methylheptane; 2,5-dimethylhexane; counterflow diffusion flame; ignition; extinction

Corresponding Author: Dr. Mani Sarathy,

Corresponding Author's Institution: LLNL

First Author: Mani Sarathy

Order of Authors: Mani Sarathy; Ulrich Niemann; Coleman Yeung; Ryan Gehmlich; Charles K Westbrook; Max Plomer; Zhaoyu Luo; Marco Mehl; William J Pitz; Kalyanasundaram Seshadri; Murray J Thomson; Tianfeng Lu

Abstract: Conventional petroleum, Fischer-Tropsch (FT), and other alternative hydrocarbon fuels typically contain a high concentration of lightly methylated iso-alkanes. However, until recently little work has been done on this important class of hydrocarbon components. In order to better understand the combustion characteristics of real fuels, this study presents new experimental data for 3-methylheptane and 2,5-dimethylhexane in counterflow diffusion flames. This new dataset includes flame ignition, extinction, and speciation profiles. The high temperature oxidation of these fuels has been modeled using an extended transport database and a high temperature skeletal chemical kinetic model. The skeletal model is generated from a detailed model reduced using the directed relation graph with expert knowledge (DRG-X) methodology. The proposed skeletal model contains sufficient chemical fidelity to accurately predict the experimental speciation data in flames. The predicted concentrations of species are compared to elucidate the effects of number and locations of the methyl branches. The location of the methyl branch is found to have little effect on ignition and extinction in these counterflow diffusion flames. However, increasing the number of methyl branches was found to inhibit ignition and promote extinction. With regards to the species composition of these counterflow flames, the location and number of methyl branches was found to particularly affect the amount and type of alkenes observed.

Submitted to 34th International Symposium on Combustion

A counterflow diffusion flame study of lightly branched octane isomers

S.M. Sarathy[1], U. Niemann[2], C. Yeung[3], R. Gehmlich[2], C.K. Westbrook[1], M. Plomer[4], Z. Luo[4], M. Mehl[1], W.J. Pitz[1], K. Seshadri[4], M.J. Thomson[3], T. Lu[4]

[1] *Lawrence Livermore National Laboratory, Physical and Life Sciences Directorate, Chemical Sciences Division, 7000 East Avenue, Livermore, California, USA*
[2] *University of California, San Diego, California USA*
[3] *University of Toronto, Department of Mechanical and Industrial Engineering, 5 King's College Road, Ontario, Canada*
[4] *University of Connecticut, Storrs, Connecticut, USA*

Corresponding author: S.M. Sarathy
7000 East Ave., L-367
Livermore, CA 94658
USA
sarathy1@llnl.gov
Ph. 925-423-6011

Colloquium: Laminar flames
Paper length: 6198 words (2 words available)
Text= 3360 (/Word processor) +
Equations=0 lines x7.6x * column=0 +
References=(15+2)x2.3x7.6= 297 +
Figures=
2 x(127+10)x2.2x2col.=*1205* +
2x(61+10)x2.2x1col.=*312* +
1x(105+10)x2.2x2col.=*506* +
1x(58+10)x2.2x2col.=*299* +
words in captions=219
=2541

Abstract length: 213 words (137 words available)

Keywords: 3-methylheptane, 2,5-dimethylhexane, counterflow diffusion flame, ignition, extinction

Abstract

Conventional petroleum, Fischer-Tropsch (FT), and other alternative hydrocarbon fuels typically contain a high concentration of lightly methylated iso-alkanes. However, until recently little work has been done on this important class of hydrocarbon components. In order to better understand the combustion characteristics of real fuels, this study presents new experimental data for 3-methylheptane and 2,5-dimethylhexane in counterflow diffusion flames. This new dataset includes flame ignition, extinction, and speciation profiles. The high temperature oxidation of these fuels has been modeled using an extended transport database and a high temperature skeletal chemical kinetic model. The skeletal model is generated from a detailed model reduced using the directed relation graph with expert knowledge (DRG-X) methodology. The proposed skeletal model contains sufficient chemical fidelity to accurately predict the experimental speciation data in flames. The predicted concentrations of species are compared to elucidate the effects of number and locations of the methyl branches. The location of the methyl branch is found to have little effect on ignition and extinction in these counterflow diffusion flames. However, increasing the number of methyl branches was found to inhibit ignition and promote extinction. With regards to the species composition of these counterflow flames, the location and number of methyl branches was found to particularly affect the amount and type of alkenes observed.

1. Introduction

The present study is concerned with the combustion of lightly branched alkanes (e.g., octane isomers), as these structures are important components of conventional and alternative transportation fuels. For example, 2,5-dimethylhexane has been reported as a component of petroleum combustion exhaust, smog, and tobacco smoke [1]. It is important to understand the high temperature combustion properties of lightly branched alkanes, including the effects of methyl branching on flame speciation profiles and counterflow flame ignition and extinction. The focus of the present work is on singly- and di-methylated C_8 alkanes because the chain length is sufficient to explore the various effects of methyl branch location and number.

Recent comprehensive experimental and modeling studies on 2-methylalkanes [2,3] have shown that singly methylated alkanes (e.g., 2-methylheptane) exhibit notably different combustion properties than their linear alkane counterparts (e.g., n-octane), including lower laminar flame speed and suppressed low temperature auto-ignition behavior. These studies need to be extended to iso-alkanes with methyl groups on different locations and with more than one methyl substitution. As a next step, the present study focuses on 3-methylheptane and 2,5-dimethylhexane. The latter dimethyl compound was chosen because of its symmetrical structure that simplifies chemical synthesis and chemical kinetic model development. Prior fundamental combustion studies on 3-methylheptane and 2,5-dimethylhexane are limited. Recently, Ji et al. [4] conducted laminar flame speed measurements of five octane isomers and compared them to chemical kinetic modeling predictions; both experimental and modeling results indicated that 3-methylheptane exhibits indistinguishable laminar flame propagation speeds when compared to 2-methylheptane, while both of them are slower than that of n-octane. Additionally, their results showed that 2,5-dimethylhexane exhibits lower laminar flames speeds than that of the singly methylated octane isomers, thereby suggesting the methyl branch location does not affect flame propagation rates, whereas the number of methyl branches does.

The objective of this study is to better understand the combustion properties of lightly branched alkanes in counterflow diffusion flames. This study presents new experimental data for 3-methylheptane and 2,5-dimethylhexane obtained in counterflow diffusion flames and compares the results with previous data obtained for 2-methylheptane [2] under similar conditions. A high temperature detailed chemical kinetic model is used to describe the oxidation chemistry of these fuels. Furthermore, the detailed model is reduced in size using the directed relation graph method with expert knowledge (DRG-X) to reduce the simulation costs, while maintaining a high degree of chemical fidelity for predicting flame ignition, extinction and intermediate species concentrations. Thus, the skeletal model is used as a tool to provide meaningful insights into the effects of methyl branching on flame structure.

2. Methodologies

2.1 Counterflow Diffusion Flame Speciation Experiments

The experimental setup at the University of Toronto is similar to that described earlier by Sarathy et al. [2], and it has been used to study a number of fuels [5-7]. The setup consists of two identical circular burner ports with a diameter of 25.4 mm, facing each other and spaced 20 mm apart. A fuel mixture of 98.14% N_2 and 1.86% fuel (98% pure 3-methylheptane or 2,5-dimethylhexane) is fed through the bottom port at a mass flux rate of 0.015 g/cm^2-sec, while an oxidizer mixture of 42.25% O_2 and 57.75% N_2 is fed through the top port at a mass flux rate of 0.014 g/cm^2-sec. The fuel-nitrogen mixture was prepared using a commercially available Bronkhorst fuel vaporization system. The temperatures of the gases exiting the top (oxidizer) and bottom (fuel) burner ports were 420 K and 350 K, respectively. The partial pressure of the fuel was below the fuel vapor pressure at 420K to ensure that the fuel was maintained in the vapor phase. The mass flow controllers used to meter the delivery of nitrogen, fuel, oxygen, and air have a manufacturer-reported-error of ±1%.

The gas sampling system in these experiments consists of a fused-silica microprobe (0.20 mm internal diameter, 0.32 mm outer diameter, and 5 cm length) connected to a dual-stage pump with

heated heads (420 K) and PTFE diaphragms to prevent the condensation of high boiling point compounds. Analytical techniques used to analyze the species in the sample include: GC/FID with an HP-Al/S PLOT column for C_1 to C_8 hydrocarbons and GC/TCD for CO and CO_2. Temperature measurements were obtained using both a 75 μm wire diameter R-type thermocouple (uncoated Pt/Pt-13%Rh) and corrected for radiation losses [2]. We estimate a maximum error of ±10% in the temperature measurements, and the precision of species measurements is estimated to be ±15%.

2.2 Counterflow Diffusion Flame Ignition/Extinction Experiments

Critical conditions of extinction and ignition of non-premixed flames were measured employing the counterflow burner at University of California, San Diego [8]. In this configuration, a fuel stream consisting of vaporized fuel (98% pure) and nitrogen is introduced through one duct, and an oxidizer stream of air is injected from the other duct. The mass fraction of fuel, the fuel stream density, temperature, and the component of the flow velocity normal to the stagnation plane at the fuel boundary are represented by $Y_{F,1}$, ρ_1, T_1, and V_1, respectively. The mass fraction of oxygen, oxidizer density, temperature, and the component of the flow velocity normal to the stagnation plane at the oxidizer boundary are represented by $Y_{O_2,2}$, ρ_2, T_2, and V_2, respectively. Diameters of both the fuel and the oxidizer ducts are 23 mm. Extinction experiments were conducted with a duct separation of L = 10mm, and T_2 = 298 K. The temperature of the fuel stream, T_1, for all fuels is 400K (±10K). At some selected value of $Y_{F,1}$, the flame was stabilized. The strain rate (see [3,8] for definition) was increased by increasing V_1 and V_2 simultaneously while keeping momenta of the counterflow streams balanced based on $\rho_1 V_1^2 = \rho_2 V_2^2$ until extinction occurred.

Ignition experiments were carried out with a duct separation of L = 12mm, a fuel stream exit temperature of 400K (±10K) , and a fuel mass fraction, $Y_{F,1}$=0.4. For a fixed strain rate a_2, the temperature at the oxidizer inlet was increased until auto-ignition took place. The velocities of the

counterflow streams were constantly adjusted based on the change in temperature for balanced momenta.

The accuracies of the strain rate and fuel mass fraction were 5% and 3% of the recorded values, respectively. The experimental repeatability of the reported strain rate at extinction was 3% of the recorded value. The accuracy of the measurement of the oxidizer temperature was determined to be ±20K. The experimental repeatability of the recorded temperature of air at auto-ignition was ±5K.

2.4 Chemical Kinetic Model Formulation

The detailed chemical kinetic mechanism includes high-temperature kinetic schemes for 3-methylheptane (C_8H_{18}-3) and 2,5-dimethylhexane (C_8H_{18}-25). The model was developed by extending a previously developed model on 2-methylheptane (C_8H_{18}-2) [3] to describe the unique oxidation chemistry of the aforementioned fuels. The complete detailed model consists of 767 species and 3961 reactions. The THERM [9] software was used to compute the thermochemical properties of the species. The transport properties were obtained following the method described by Sarathy et al. [3].

2.4 Mechanism Reduction with DRG-X

The method of direct relation graph (DRG) with expert knowledge (DRG-X) [10-12] was employed to eliminate unimportant species and reactions in the detailed mechanism. Compared with the original DRG method that is limited by a uniform error tolerance for every species, DRG-X allows the specification of non-uniform error tolerances for different species and heat release (i.e., the expert knowledge). As such, DRG-X can generate smaller skeletal mechanisms with similar chemical fidelity compared with DRG. Procedurally, in addition to the starting species (e.g., the H radical), species-specific x-values (i.e., error tolerances) are specified for selected species based on expert knowledge. A species, A, associated with reactions with small uncertainties can be assigned a

small x-value, say x_A=0.1, while that with larger uncertainties can be assigned a larger x-value, say x_A=0.5. Any species B with (see [10] for definition of) will be retained in the skeletal mechanism, while other species are treated with the original DRG reduction using a default error tolerance, say ε=0.7. As a result the errors in the skeletal mechanisms roughly match the level of uncertainties in the detailed mechanisms, such that the overall chemical fidelity can be retained. Moreover, smaller x-values can be specified for some species of interest (e.g., a pollutant), which need to be predicted with higher accuracy than other species. This is particularly important in the present work because low x-values are needed to properly predict the intermediate species measured in the flame structure experiments.

The reduction was performed based on reaction states sampled from auto-ignition and perfectly stirred reactors (PSR) in a parameter range that is relevant to the counterflow flames in the present work. That is the atmospheric pressure, equivalence ratios between 0.5 and 2.0, initial temperature for auto-ignition of 1200–1800 K, and inlet temperature of 300 K for PSR, which gave reactor temperatures of 1000–2300 K for 1 atm and the stoichiometry considered. By setting an error tolerance of 0.3 for all the species measured in the counterflow flame speciation experiments (refer to Table S1), an error tolerance of 0.01 for heat release, and a default error tolerance of ε=0.95 for all the other species, a skeletal mechanism consisting of 241 species and 1587 reactions was obtained.

3. Results and Discussion

3.1 Counterflow Diffusion Flame Speciation Results

The measured species in the counterflow diffusion flame speciation experiments are shown in Figures 1 and 2 and Table S2. The gas chromatography method could not separate 1-butene (1-C_4H_8) from 1,2-propadiene (1,2-C_3H_4), so we report the combined concentration of these two species. The same was done for 1,3-butadiene (1,3-C_4H_6) and propyne (C_3H_4). The reported species and temperature profiles were shifted by 0.305 mm away from the fuel port to account for a

positioning uncertainty, which is a human error introduced when zeroing the sampling probe against the fuel port surface. The skeletal mechanism was used to predict the counterflow flame speciation and temperature profiles using the OPPDIF solver in CHEMKIN PRO [13] with mixture-averaged transport and thermal diffusion (GRAD 0.1, CURV 0.1). The converged solution contained approximately 300 grid points, and was verified to be grid-size independent.

Figure 1 displays the measured and predicted species profiles obtained in the 3-methylheptane counterflow diffusion flame. Besides CO and CO_2, the most abundant measured species are C_2H_4, C_2H_2, CH_4, and C_3H_6. The skeletal model well reproduces the shape of the experimental species profiles. In general, the peak of the profiles are accurately reproduced by the model, being significantly better than that presented previously for 2-methylheptane and n-octane [2]. This is attributed to a new commercial fuel vaporization system (Bronkhorst) that allows more careful flow control and mixing of the fuel and nitrogen diluent gas. In the following discussion, the model's quantitative prediction is considered good if the predicted maximum mole fraction is within a factor 1.5 of the measured maximum mole fraction. Table S2 in the supplementary material presents the predicted and measured maximum mole fractions, as well as their ratio.

Temperature profiles presented in the supplementary material Fig. S1 indicate that the skeletal model predicted the experimental measurements remarkably well. A slight delay (i.e., shift away from the fuel port) in the predicted reactivity of 3-methylheptane is observed in Fig. 1, while the model performs well in predicting the peak concentrations of CO, CO_2, CH_4, C_2H_4, C_2H_2, C_2H_6, C_3H_6, 1,3-C_4H_6 + C_3H_4, iC_4H_8, 1-C_4H_8 + 1,2-C_3H_4, and 2-C_4H_8.

Figure 2 displays the measured and calculated species profiles in the 2,5-dimethylhexane counterflow diffusion flame, and temperature profiles are presented in the supplementary material Fig. S2. The measured profiles of the fuel, CO, CO_2, and temperature are comparable to those of 3-methylheptane. The model well predicts the experimentally measured profile for temperature and

2,5-dimethylhexane, and the peak concentrations of CO and CO_2, CH_4, C_2H_4, C_2H_6, C_3H_6, 1,3-C_4H_6 + C_3H_4, iC_4H_8, and 1-C_4H_8 + 1,2-C_3H_4, while the peak mole fraction of C_2H_2 was over-predicted by a factor of 1.5.

Experiments and simulations were compared to elucidate the differences in combustion between the three lightly branched C_8 isomers. Comparisons were made for data obtained for 2-methylheptane, 3-methylheptane, and 2,5-dimethylhexane under identical fuel and oxidizer boundary conditions. Table S2 in the supplementary material presents the peak measured and predicted mole fractions in the three flames. Considering that the experimental error is ±15%, all flames have similar concentrations of CO_2, CO, CH_4, C_2H_6, and C_2H_2. As the methyl branch moves from the second to the third carbon (i.e., 2-methylheptane to 3-methylheptane) there is a decrease in iso-butene production and an increase in 1-butene and 2-butene production. The C_3H_6 and C_2H_4 are comparable between 2-methylheptane and 3-methylheptane flames. The 2,5-dimethylhexane flame produces the least amount of C_2H_4 and greatest amounts of C_3H_6 and iso-butene compared to the other flames.

3.1 Counterflow Diffusion Flame Extinction/Ignition Results

The skeletal mechanism was used to compute critical conditions of extinction and ignition, and the results were compared to the experiments. The extinction computations were carried out using extinction solver in CHEMKIN PRO [13], which uses the arc length continuation method to generate the S-curve. A stable flame was first obtained using the OPPDIF code at velocities near the extinction limit, and the solution was supplied as the initial guess to the extinction solver with plug flow conditions at both boundaries. The 2-point extinction method was employed with mixture-averaged transport, thermal diffusion, and convergence parameters of GRAD=0.1 and CURV=0.2.

Ignition calculations were performed using the OPPDIF solver in CHEMKIN PRO [13] using the following procedure. A fully resolved temperature profile was initially computed with cold mixtures at both inlets. The temperature of air inlet, T_2, was then slowly increased until ignition took place.

The composition of the reactant streams, their inlet flow velocities and the value of the fuel stream temperature, T_1, were all maintained constant during this procedure. The simulation employed mixture-averaged transport, thermal diffusion, and convergence parameters of (GRAD=0.1 and CURV=0.1).

Figure 3 shows the temperature of air inlet at ignition, $T_{2,I,}$ as a function of the strain rate, a_2, for values of $Y_{F,1}$ = 0.4. The results for 3-methylheptane and 2,5-dimethylhexane are shown and compared with data previously obtained for 2-methylheptane under identical conditions. The symbols represent experimental data with radiation corrected temperatures and the line represents modeling predictions. Considering the uncertainty on the temperature measurements, the model predictions are considered to be good. It is also interesting to note that the experimental an ignition temperatures for 3-methylheptane and 2-methylheptane are practically indistinguishable, suggesting that methyl branch location has a minimal effect on the ignition of counterflow diffusion flames. However, the ignition temperature for 2,5-dimethylhexane is approximately 10 K higher at the highest strain rates. This feature of decreased autoignition temperature with increased methyl branching is well reproduced by the proposed model. Smallbone et al. [14] showed that the auto-ignition temperature of n-heptane is sensitive to fuel diffusion; however, in this study chemical kinetic differences are responsible for the observed differences in autoignition temperature because the three octane isomers have virtually identical transport properties.

Figure 4 shows the mass fraction of fuel, $Y_{F,1}$, as a function of the strain rate at extinction, $a_{2,e}$. The symbols in this figure represent experimental data for the three branched alkanes. The data suggests that the extinction strain rate for 3-methylheptane and 2-methylheptane are virtually identical, and the model is able to reproduce this behaviour. However, both the model and the experimental data indicate that 2,5-dimethylhexane is slightly less reactive than its singly methylated analogues, wherein lower extinction strain rates are observed for the same fuel mass fractions.

Won et. al [15] explain that a fuel's transport-weighted enthalpy (TWE) can be used to normalize the chemical kinetic contributions to flame extinction. The fuels studied herein have the same TWE, so any observed differences in reactivity are attributed to chemical kinetic variations. Furthermore, Won et al. introduce a radical index (RI) term to quantify the kinetic contribution of fuel chemistry, which is based on the ability of a candidate fuel to populate the OH or H radical concentration within the flame structure relative to an alkane. Following their logic, we conducted numerical simulations at fixed boundary temperature conditions [15], TWE (~1.5), and strain rate (~150 s^{-1}) to estimate an RI_{OH} and RI_H for the three fuels studied herein with n-octane as the baseline fuel. Our results indicate that 2-methylheptane and 3-methylheptane have the same RI_{OH} (~ 0.97), while that of 2,5-dimethylhexane (~ 0.95) is slightly lower. An RI based on H radical concentration yields a larger difference for 3-methylheptane and 2-methylheptane (RI_H ~ 0.96) compared to 2,5-dimethylhexane (RI_H ~ 0.91), which better rationalizes the observed differences in extinction strain rate.

3.2 Reaction Path Analysis

Reaction path analyses were performed using the proposed model to explain the difference observed for the 2-methylheptane, 3-methylheptane, and 2,5-dimethylhexane flames measured at the University of Toronto. Reaction path analyses were performed at two different temperatures, 805 K and 1185 K, which are the same conditions presented previously for 2-methylheptane [2].

Figure 5 displays the primary reaction paths involved in the consumption of 3-methylheptane at the two aforementioned temperatures, with italic and bold texts referring to low and high temperature conditions, respectively. According to the proposed model, H-atom abstraction accounts for most of the fuel consumption, while 30% of 3-methylheptane is consumed via unimolecular decomposition reactions (not shown in figure) at the higher temperature. At both low and high temperatures, H-atom abstraction from the tertiary carbon is the most predominant route (20%). The fuel radicals formed via H-atom abstraction are primarily consumed via β-scission. However, radical

isomerization reactions to the tertiary site via 5- and 6-membered transition state rings are also important.

Figure 6 shows the reaction paths involved in the consumption of 2,5-dimethylhexane, which is a symmetric molecule. At both low and intermediate temperatures, H-atom abstraction accounts for nearly all of the fuel consumption, with unimolecular decomposition of minor importance at the lower temperature. The fuel radicals formed are primarily consumed via β-scission reactions. However, at both temperatures most of the primary radical (C_8H_{17}-25a) radical undergoes isomerization to form the tertiary radical (C_8H_{17}-25b) via a 6-membered transition state. The fuel radicals undergo β-scission reactions and produces iso-butene, propene, and large branched alkenes.

As mentioned previously, the 2,5-dimethylhexane flame produces more iso-butene and propene than the singly methylated alkanes, which is rationalized by the high flux through the tertiary fuel radical. The 3-methylheptane flame produces more 1-butene and 2-butene than the 2-methylheptane flame, which favors iso-butene formation. This is rationalized by the positioning of the methyl branch, which leads to various butenes upon fuel radical decomposition.

4. Conclusions

The present study presented new experimental data for 3-methylheptane and 2,5-dimethylhexane obtained in counterflow diffusion flames. The experimental results along with kinetic modeling simulations were used to elucidate the effects of the number and locations of the methyl branches on flame structures. The kinetic modeling simulations were conducted using a skeletal mechanism generated using the DRG-X algorithm. Both the experimental data and the model suggested that increasing number of methyl branches in a molecule increases the production of iso-butene and decreases the formation of ethylene and propene. The locations of the methyl branches also affect the relative amounts of 1-butene, 2-butene, and iso-butene. However, methyl branch location did not significantly change the extinction and ignition limits of counterflow diffusion flames, whereas the

number of methyl branches did. The changes observed with increased methyl branching can be attributed to the fuel's ability to populate the H radical concentration.

5. Acknowledgements

We are thankful to Sang Hee Won for fruitful discussions. This work performed under the auspices of the U.S. Department of Energy by Lawrence Livermore National Laboratory under Contract DE-AC52-07NA27344. LLNL also acknowledges the support of the US Department of Energy, Office of Vehicle Technologies (program manager Gurpreet Singh) and the Office of Naval Research (program manager Sharon Beermann-Curtin). The research at the University of California at San Diego is supported by the U.S Army Research Office Grant # W911NF-09-1-0108 (Program Manager Dr Ralph A. Anthenien Jr). The co-authors SMS, CY, and MJT acknowledge support from NSERC of Canada. The work at University of Connecticut was supported by the National Science Foundation under Grant 0904771.

6. Supplementary Material

The 241 species skeletal model with corresponding thermodynamic and transport data in CHEMKIN format is provided as supplementary material.

7. References

1. M. Serve, D. Bombick, J. Roberts, G. McDonald, Chemosphere 22 (1991) 77-84.
2. S.M. Sarathy, C. Yeung, C.K. Westbrook, W.J. Pitz, M. Mehl, M.J. Thomson, Combust. Flame 158 (2010) 1277–1287.
3. S.M. Sarathy, C.K. Westbrook, M. Mehl, W.J. Pitz, C. Togbe, P. Dagaut, H. Wang, M.A. Oehlschlaeger, U. Niemann, K. Seshadri, P.S. Veloo, C. Ji, F.N. Egolfopoulos, T. Lu, Combust. Flame 158 (2011) 2338–2357.
4. C. Ji, S.M. Sarathy, P.S. Veloo, C.K. Westbrook, F.N. Egolfopoulos, Combust. Flame (2011) accepted, in press.

5. S.M. Sarathy, M.J. Thomson, W.J. Pitz, T. Lu, Proc. Combust. Inst. 33 (2011) 399–405.
6. G. Dayma, S.M. Sarath , C. Yeung, M. Thomson, P. Dagaut, Proc. Combust. Inst. 33 (1) (2011) 1037–1043.
7. S.M. Sarathy, M.J. Thomson, C. Togbé, P. Dagaut, F. Halter, C. Mounaim-Rousselle, Combust. Flame 156 (2009) 852–864.
8. K. Seshadri, T.F. Lu, O. Herbinet, S.B. Humer, U. Niemann, W.J. Pitz, R. Seiser, C.K. Law, Proc. Combust. Inst. 32 (2009), 1067-1074.
9. E. Ritter, J. Bozzelli, Int. J. Chem. Kinet. 23 (1991) 767–778.
10. T.F. Lu, C.K. Law, Proc. Combust. Inst. 30 (2005), 1333-1341.
11. Z. Luo, T.F. Lu, M.J. Maciaszek, S. Som, and D.E. Longman, Ener. Fuel. 24 (2010), 6283–6293.
12. T. Lu, M. Plomer, Z. Luo, S.M. Sarathy, W.J. Pitz, S. Som, D.E. Longman, 2011 7th US Nat'l Combust. Meet. (2011) 1–10.
13. CHEMKIN-PRO Release 15101, Reaction Design, Inc., San Diego, CA, 2010.
14. A. Smallbone, W. Liu, C. Law, X. You, H. Wang, Proc. Combust. Inst. 32 (2009) 1245–1252.
15. S.H. Won, S. Dooley, F.L. Dyer, Y. Ju, Combust. Flame. (2011) doi:10.1016/j.combustflame.2011.08.020

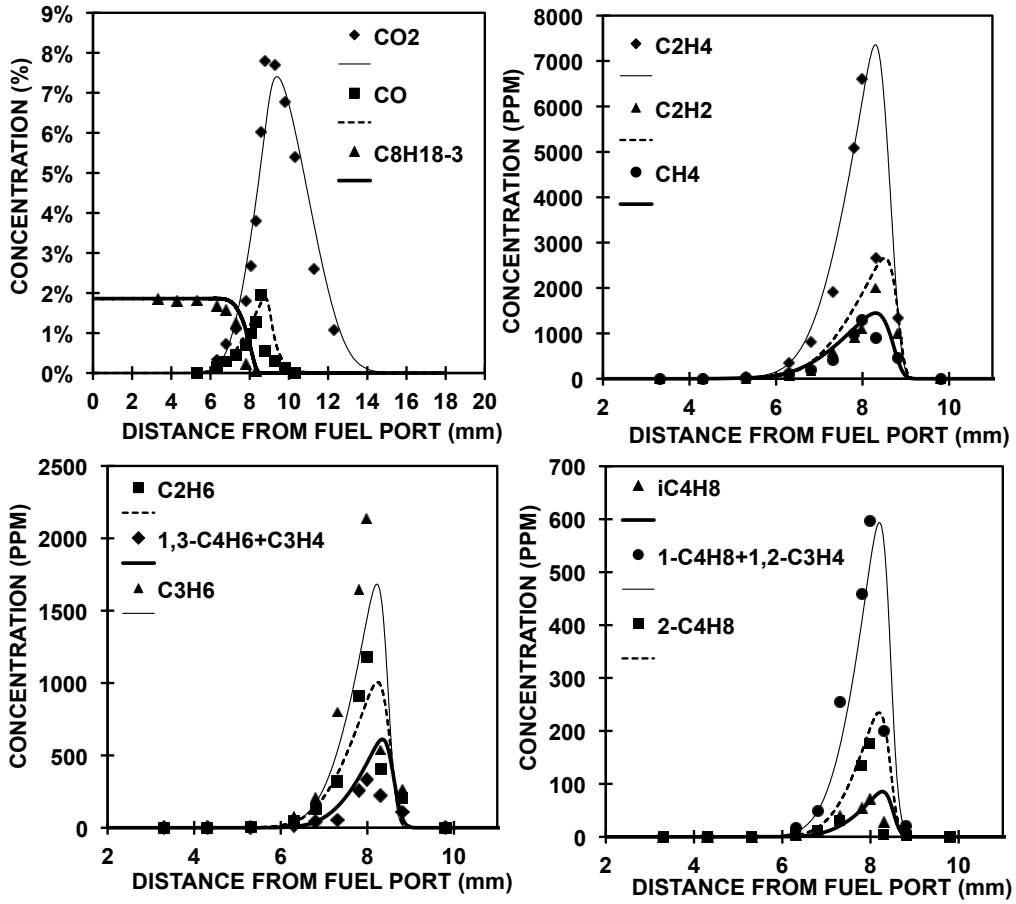

Figure 1 - Experimental and computed species concentration profiles for the oxidation of 3-methylheptane in a counterflow diffusion flame at atmospheric pressure (1.86% fuel, 42% O_2).

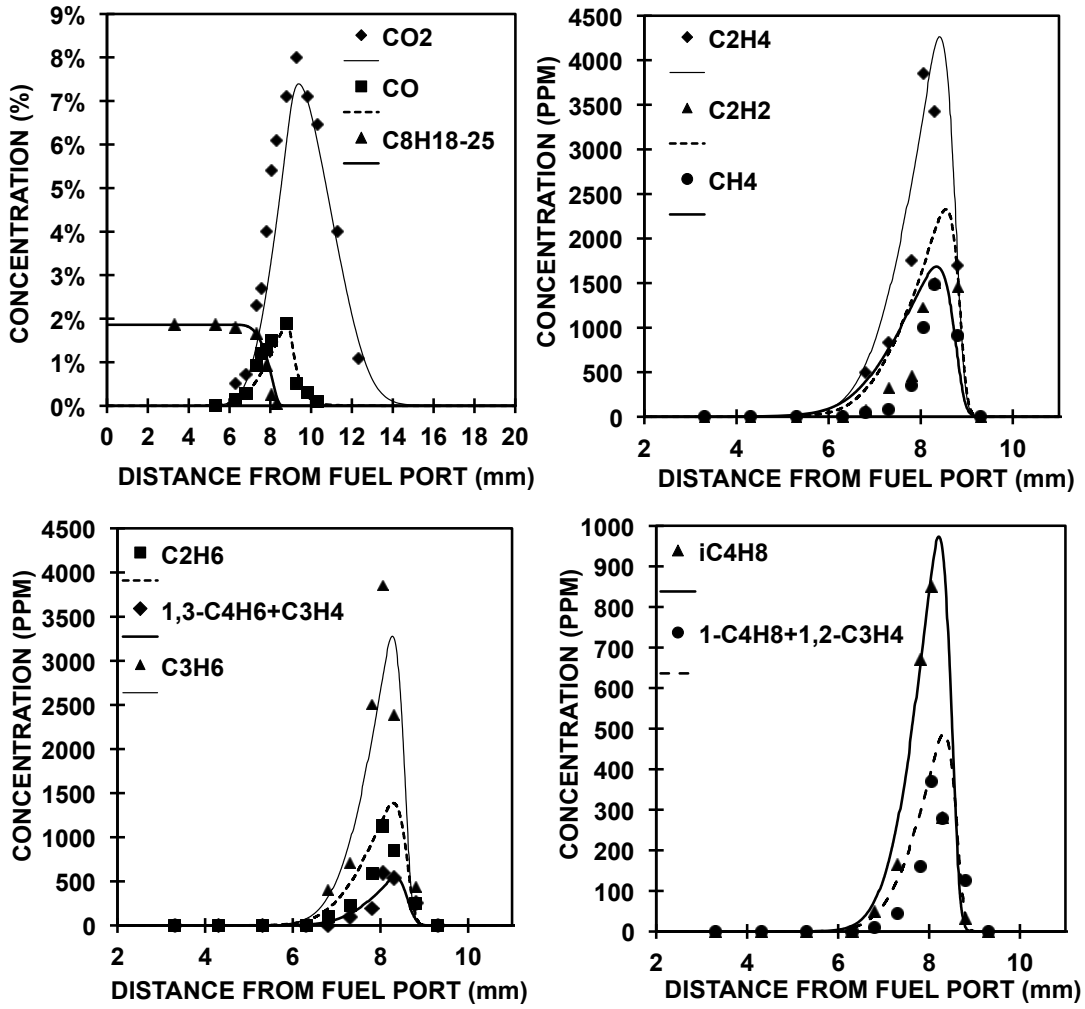

Figure 2 - Experimental and computed species concentration profiles for the oxidation of 2,5-dimethylhexane in a counterflow diffusion flame at atmospheric pressure (1.86% fuel, 42% O_2).

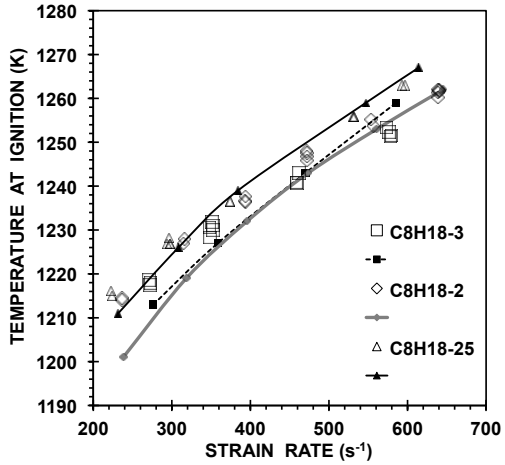

Figure 3 - The temperature at the air inlet at ignition, $T_{2,I}$, as a function of the strain rate, a_2, for $Y_{F,1}$ = 0.4 in the counterflow diffusion flame. Open symbols are experimental data and curves with closed symbols are modeling predictions.

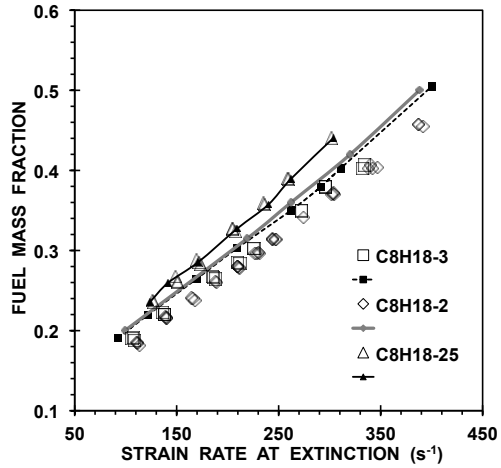

Figure 4 - The mass fraction of fuel, $Y_{F,1}$, as a function of the strain rate at extinction, $a_{2,e}$ in the counterflow flame. Results for the experiments are open symbols and from the model are open symbols with curves.

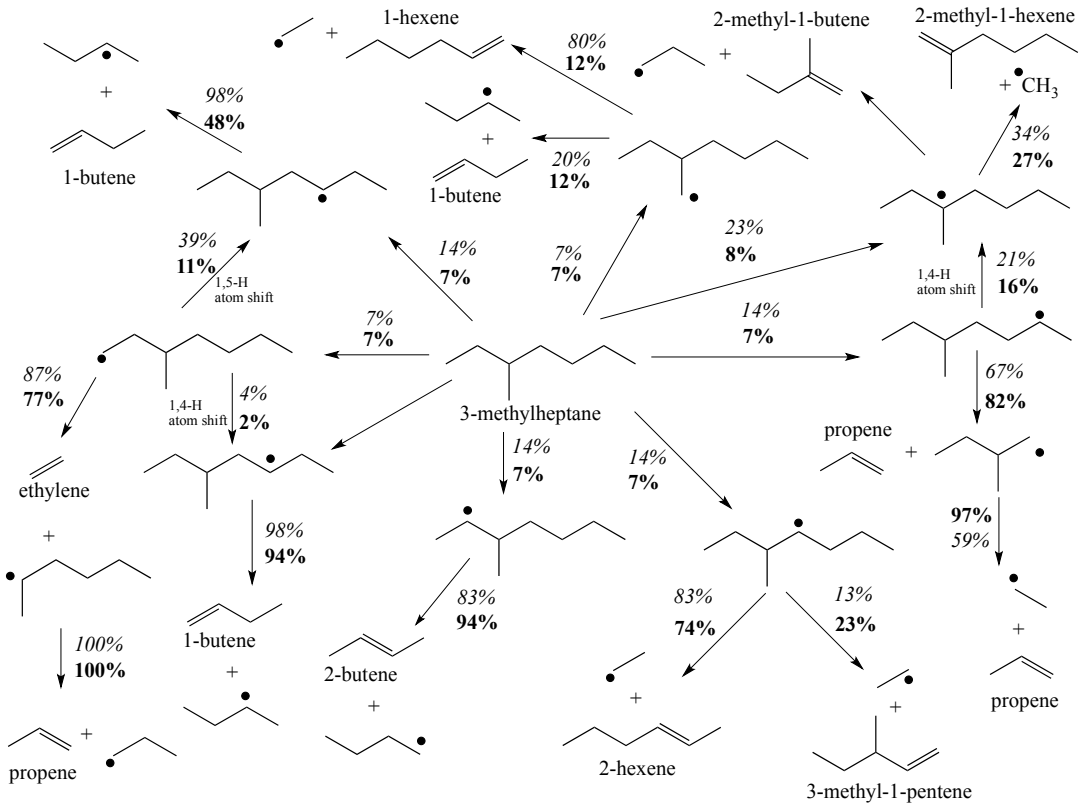

Figure 5 - Reaction pathway diagram for 3-methylheptane oxidation in the Univ. of Toronto counterflow diffusion flame at T = 805 K (italicized text) and T = 1185 K (bold text). Percentages are the net % fluxes form the source to target species.

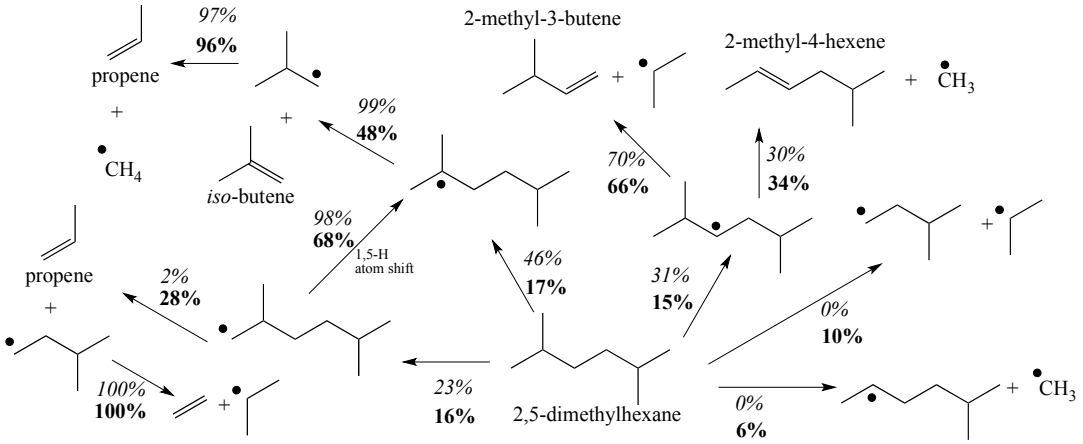

Figure 6 - Reaction pathway diagram for 2,5-dimethylhexane oxidation in the Univ. of Toronto counterflow diffusion flame at T = 805 K (italicized text) and T = 1185 K (bold text). Percentages are the net % fluxes form the source to target species.

Table S1 – Error tolerances specified for temperature and species of interest in DRG-X

Target Parameter/Species	Error Tolerance
Temperature (T)	0.01
H	0.3
OH	0.3
CH_3	0.3
C_8H_{18}-2	0.3
C_8H_{18}-3	0.3
C_8H_{18}-25	0.3
CO_2	0.3
CO	0.3
CH_4	0.3
C_2H_4	0.3
C_2H_2	0.3
C_3H_6	0.3
iC_4H_8	0.3
C_4H_8-1	0.3
C_4H_8-2	0.3
pC_3H_4	0.3
1,3-C_4H_6	0.3

Table S2- Peak measured and predicted temperatures and concentrations in the counterflow diffusion flames. Italicized numbers are measured values, bold numbers represent predicted values, and underlined numbers are the ratio of measured to predicted.

Measured Parameter	C_8H_{18}-2	C_8H_{18}-3	C_8H_{18}-25
Temperature (K)	*1688* 1604 1.0	*1604* 1633 1.0	*1572* 1604 1.0
CO_2 / carbon dioxide (%)	*7.70* 7.45 1.0	*7.80* 7.40 1.0	*8.00* 7.36 0.92
CO / carbon monoxide (%)	*2.30* 1.70 1.4	*1.96* 1.86 1.4	*1.90* 1.87 1.0
CH_4 / methane (PPM)	*1368* 1261 1.1	*1284* 1446 1.2	*1482* 1595 1.1
C_2H_6 / ethane (PPM)	*827* 833 1.0	*1181* 1007 1.3	*1127* 1387 1.0
C_2H_4 / ethylene (PPM)	*6763* 6146 1.1	*6604* 7238 1.2	*3429* 4219 1.1
C_2H_2 / acetylene (PPM)	*1575* 1987 0.8	*2004* 2657 0.7	*1503* 2308 0.7
C_3H_6 / propene (PPM)	*2314* 1646 1.4	*2138* 1680 1.7	*3854* 3223 1.4
1-C_4H_8 + 1,2-C_3H_4 / 1-butene + 1,2-propadiene (PPM)	*324* 400 0.81	*596* 632 1.0	*370* 400 0.81
1,3-C_4H_6 + C_3H_4 / 1,3-butadiene + propyne (PPM)	*376* 358 1.1	*334* 637 0.8	*597* 487 1.1
iC_4H_8 / *iso*-butene (PPM)	*431* 480 0.9	*72* 88 0.8	*850* 967 0.9
C_4H_8-2/ *2*-butene (PPM)	*< LOD* N/A N/A	*175* 235 0.7	*< LOD* N/A N/A

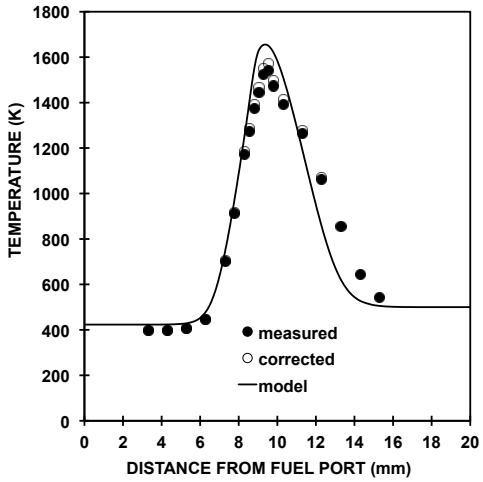

Figure S1 - Experimental and computed temperature profiles for the oxidation of 2,5-dimethylhexane in a counterflow diffusion flame at atmospheric pressure (1.86% fuel, 42% O_2).

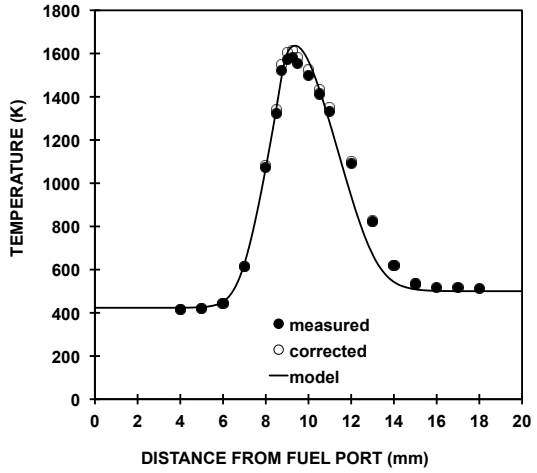

Figure S2 - Experimental and computed temperature profiles for the oxidation of 2,5-dimethylhexane in a counterflow diffusion flame at atmospheric pressure (1.86% fuel, 42% O_2).

fig s1

Click here to download Supplemental Material: fig s1 3mhp temp.pdf

fig s2

Click here to download Supplemental Material: fig s2 25dmhx temp.pdf

thermo data file

Click here to download Supplemental Material: c8_2m_3m_nalk_dimeth_v2_therm.dat

transport data file

Click here to download Supplemental Material: c8_3methylalkanes_c8_2methylalkanes_c8_c16_nalkanes_tran.dat

skeletal mechanism file

Click here to download Supplemental Material: sk241v2.txt

fig 1

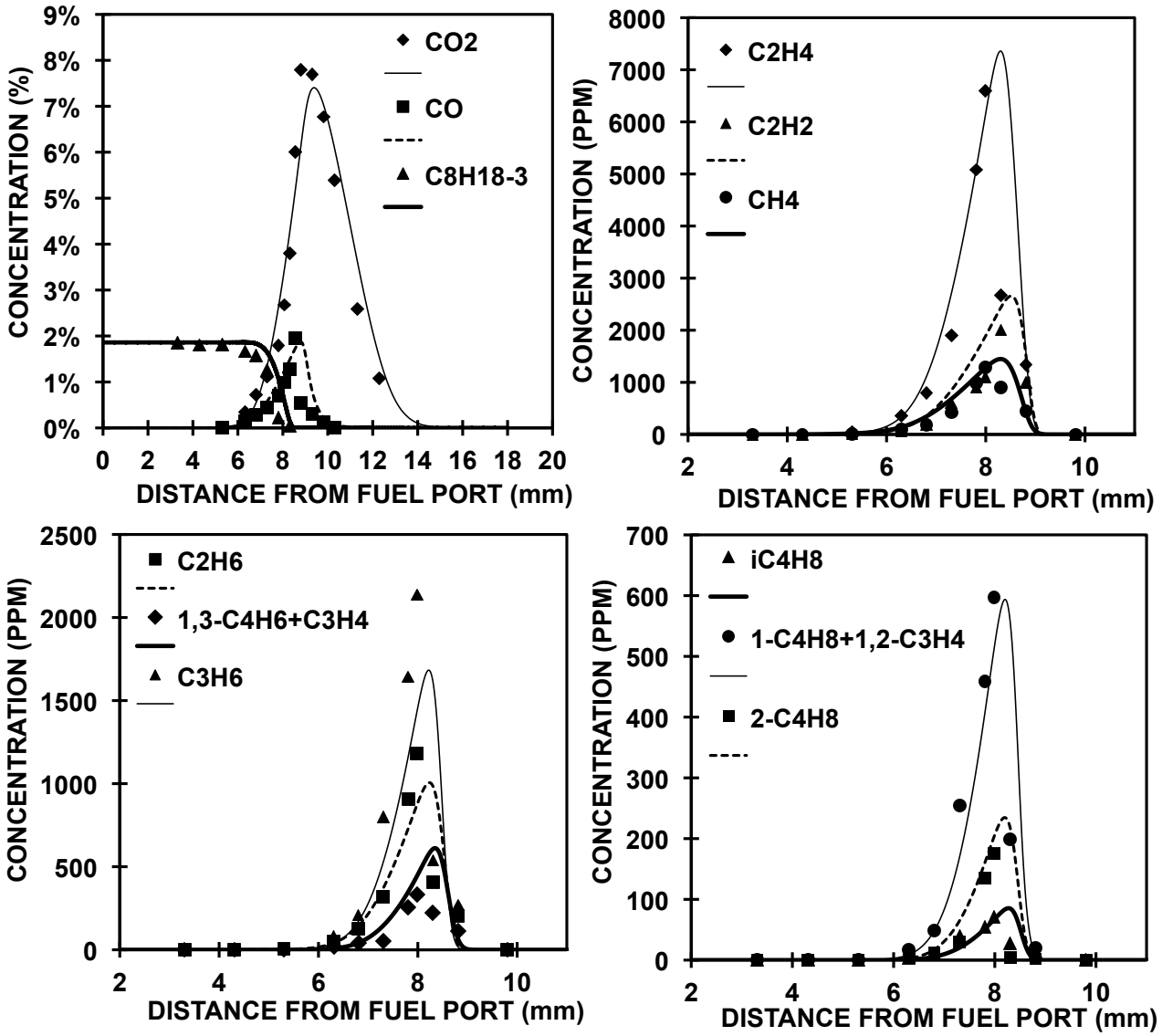
CONCENTRATION (%)
DISTANCE FROM FUEL PORT (mm)
CO2
CO
C8H18-3
CONCENTRATION (PPM)
C2H4
C2H2
CH4
C2H6
1,3-C4H6+C3H4
C3H6
iC4H8
1-C4H8+1,2-C3H4
2-C4H8

fig 2

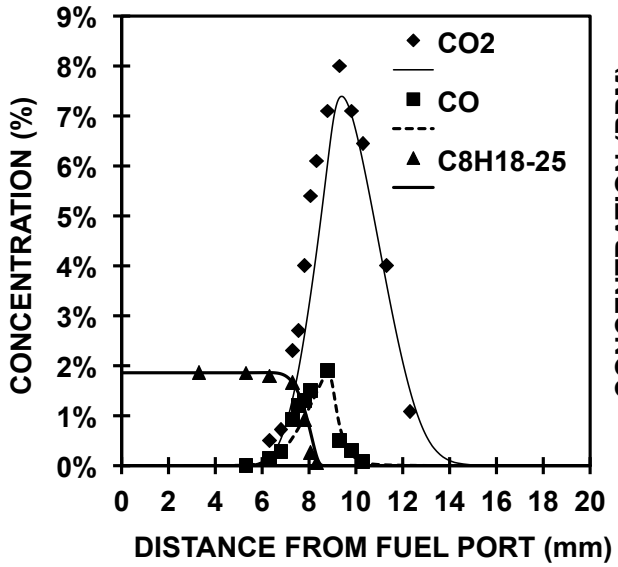
CO2
CO
C8H18-25
CONCENTRATION (%)
DISTANCE FROM FUEL PORT (mm)

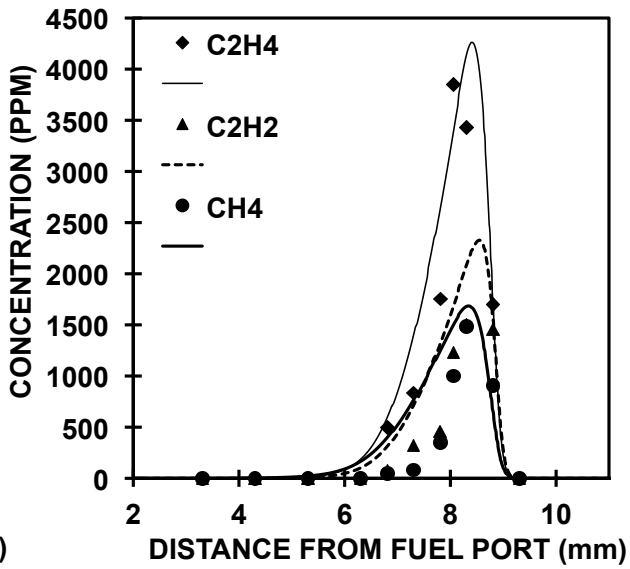
C2H4
C2H2
CH4
CONCENTRATION (PPM)
DISTANCE FROM FUEL PORT (mm)

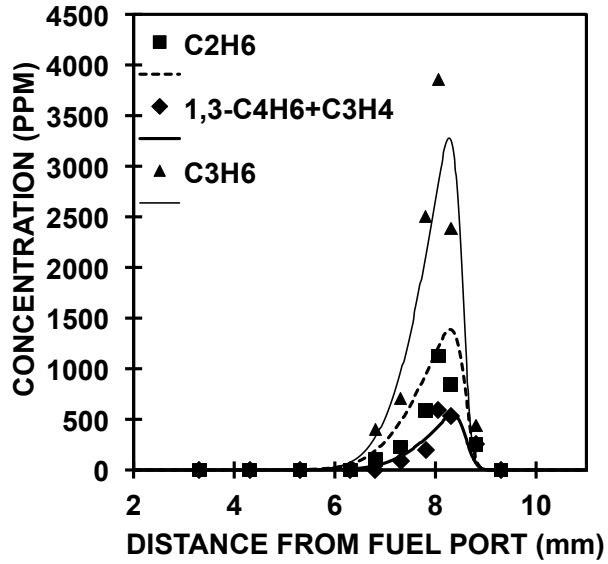
C2H6
1,3-C4H6+C3H4
C3H6
CONCENTRATION (PPM)
DISTANCE FROM FUEL PORT (mm)

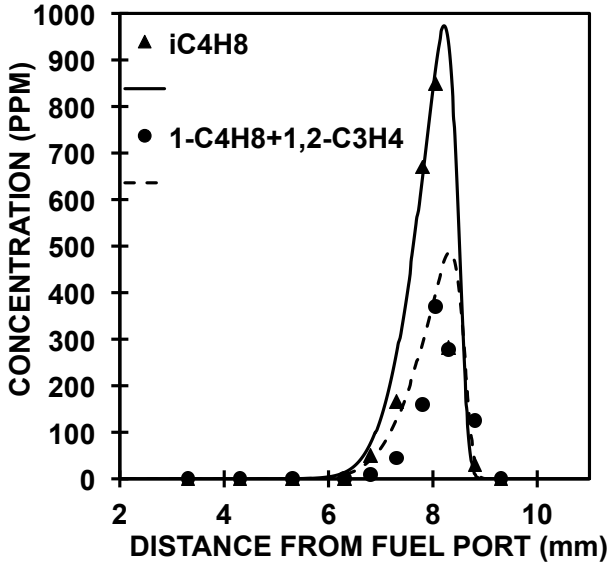
iC4H8
1-C4H8+1,2-C3H4
CONCENTRATION (PPM)
DISTANCE FROM FUEL PORT (mm)

fig 3

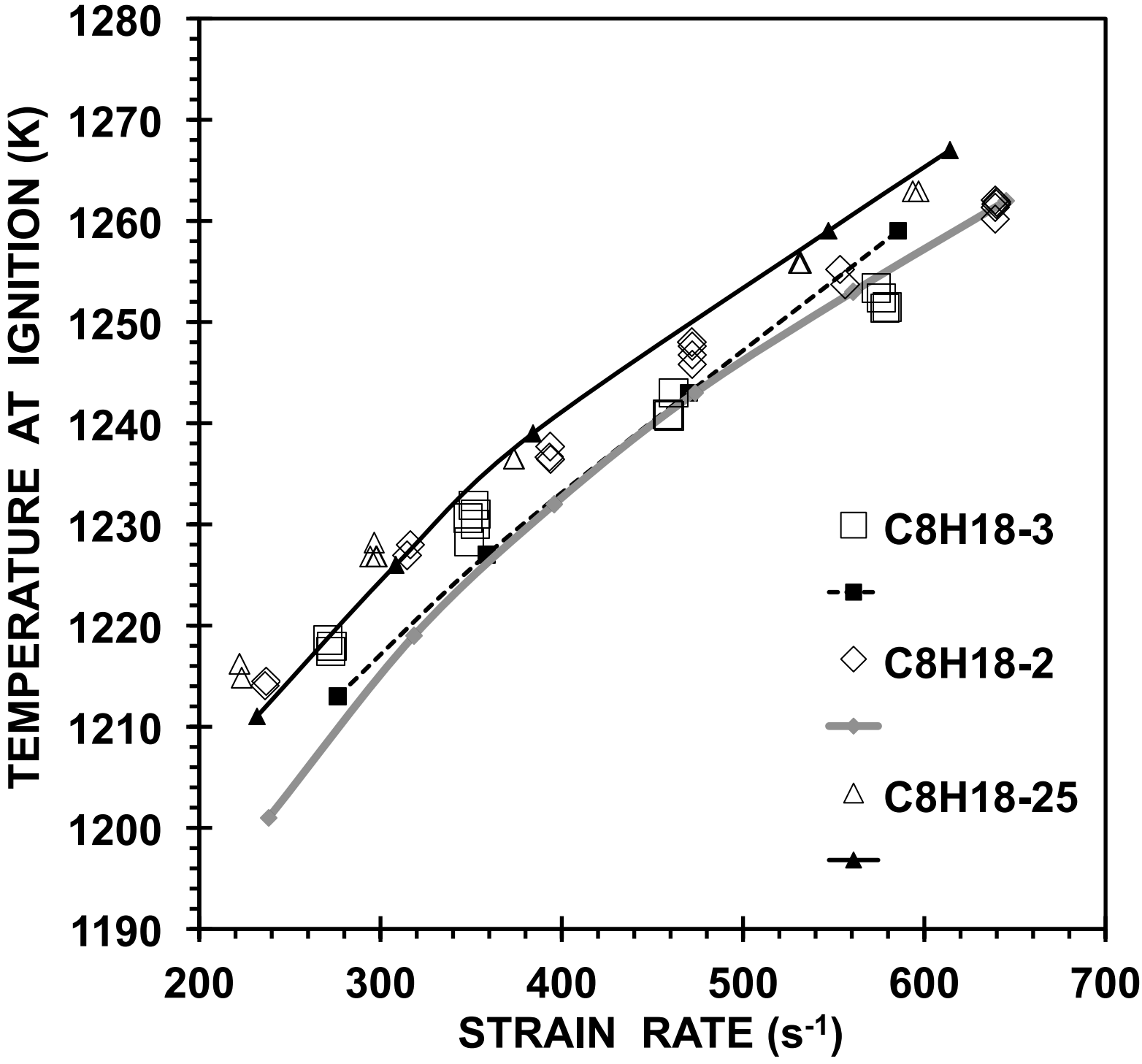
TEMPERATURE AT IGNITION (K)
1280
1270
1260
1250
1240
1230
1220
1210
1200
1190
200
300
400
500
600
700
STRAIN RATE (s-1)
C8H18-3
C8H18-2
C8H18-25

fig 4

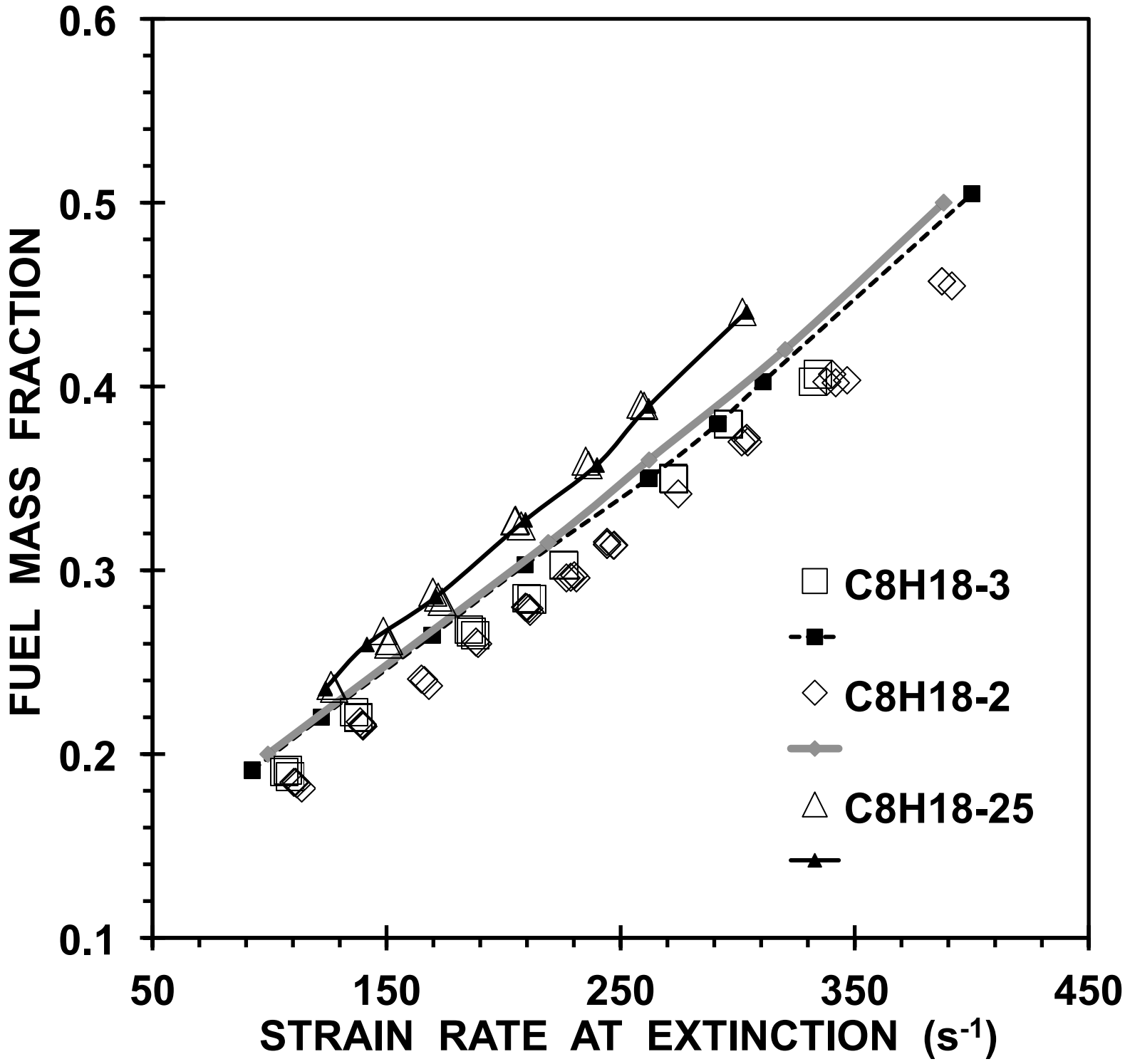
0.6
0.5
0.4
0.3
0.2
0.1
FUEL MASS FRACTION
50
150
250
350
450
STRAIN RATE AT EXTINCTION (s-1)
C8H18-3
C8H18-2
C8H18-25

fig 5

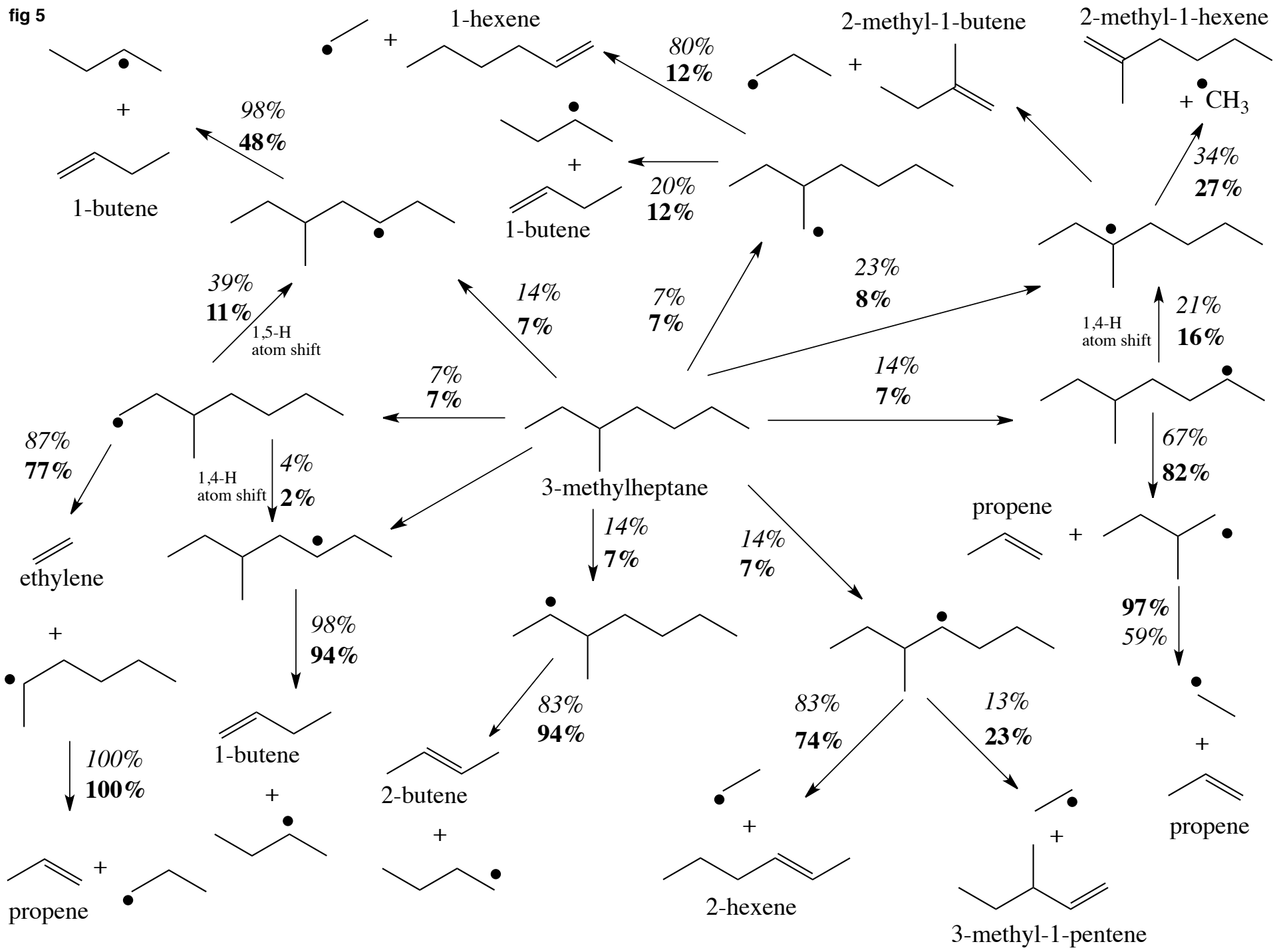
3-methylheptane
1-hexene
80%
12%
2-methyl-1-butene
2-methyl-1-hexene
+ CH3
34%
27%
98%
48%
1-butene
20%
12%
1-butene
39%
11%
1,5-H
atom shift
14%
7%
7%
7%
23%
8%
1,4-H
atom shift
21%
16%
7%
7%
14%
7%
87%
77%
1,4-H
atom shift
4%
2%
67%
82%
ethylene
propene
14%
7%
14%
7%
97%
59%
98%
94%
83%
94%
83%
74%
13%
23%
100%
100%
1-butene
2-butene
propene
2-hexene
propene
3-methyl-1-pentene

fig 6

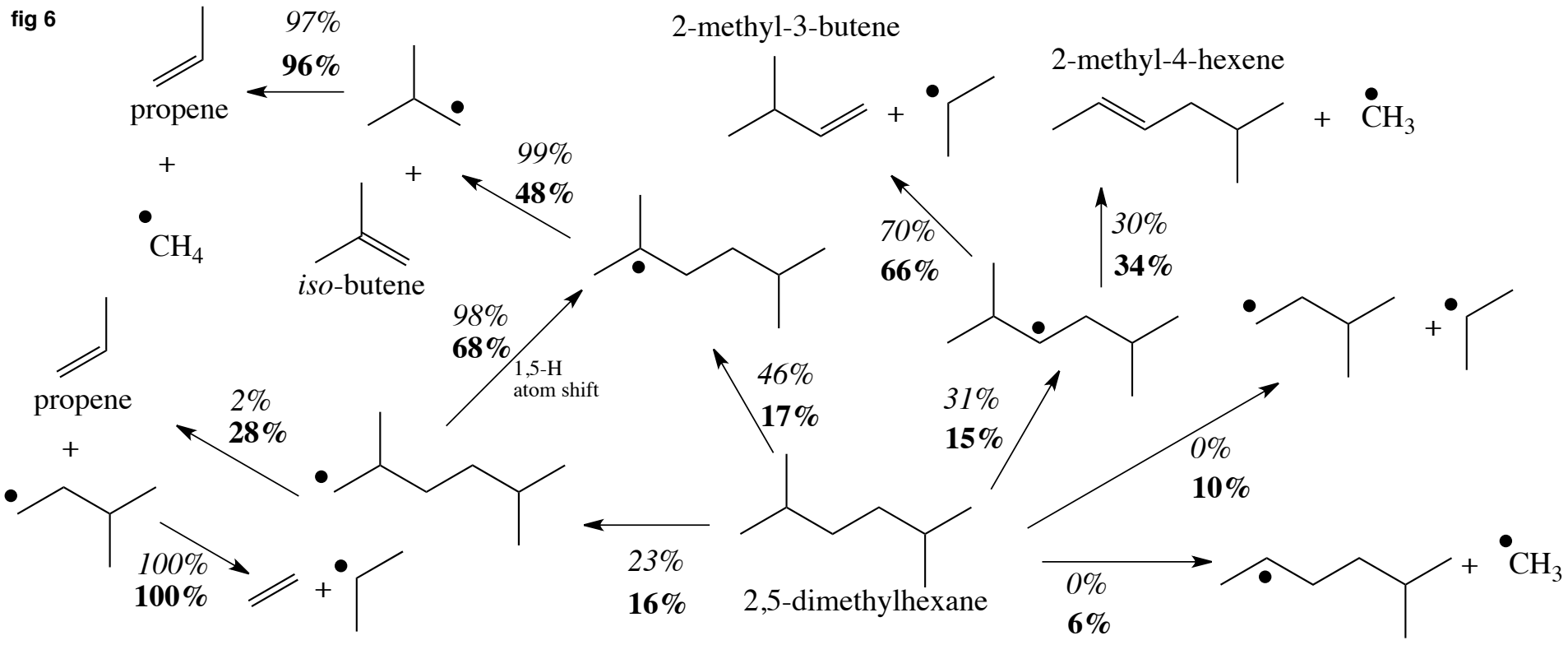
97%
96%
propene
+
CH4
+
99%
48%
iso-butene
2-methyl-3-butene
+
2-methyl-4-hexene
+
CH3
70%
66%
30%
34%
98%
68%
1,5-H
atom shift
46%
17%
31%
15%
0%
10%
propene
+
2%
28%
100%
100%
+
23%
16%
2,5-dimethylhexane
0%
6%
+
CH3